THE ASTROPHYSICAL JOURNAL, 299:741–744, 1985 December 15

STUDIES OF HOT B SUBDWARFS. IV. RADIATIVE FORCES, MASS LOSS, AND METAL ABUNDANCES IN sdB STARS

G. MICHAUD, P. BERGERON, F. WESEMAEL, AND G. FONTAINE
Département de Physique and Observatoire du mont Mégantic, Université de Montréal
Received 1985 April 26; accepted 1985 June 10

ABSTRACT

The abundance anomalies generated by diffusion in the envelopes of hot, hydrogen-rich subdwarfs are studied. It is shown that unimpeded diffusion cannot lead to the large silicon underabundance observed in those stars at effective temperatures above 30,000 K. Calculations of diffusion of heavy elements in the presence of mass loss are also performed. For a mass-loss rate of $2.5 \times 10^{-15}\ M_\odot\ \mathrm{yr}^{-1}$, the observed abundance patterns of C, N, and Si are reproduced on a time scale $\approx 10^5$ yr. Lower mass-loss rates would necessitate longer time scales. The pattern of abundance anomalies may eventually be used to constrain both the mass-loss rate and the stellar lifetime in the sdB evolutionary phase.

Subject headings: diffusion — stars: abundances — stars: early-type — stars: subdwarfs

I. INTRODUCTION

Recent high-dispersion *IUE* observations of hot, hydrogen-rich subdwarfs have revealed the existence of abundance anomalies in these objects. Particularly striking are the large underabundances of silicon (by more than a factor of 10^4) observed in sdB and sdOB stars with effective temperatures in the range 30,000–40,000 K (Baschek *et al.* 1982; Baschek, Höfflich, and Scholz 1982; Heber *et al.* 1984*a*; Lamontagne *et al.* 1985). Nitrogen seems to have approximately its solar abundance (within a factor of about 4), while carbon is generally underabundant but with significant variations from object to object. On the other hand, the cooler B subdwarfs ($T_e < 30{,}000$ K) appear to have normal abundances of C, N, and Si (Baschek and Norris 1970; Baschek, Sargent, and Searle 1972; Heber *et al.* 1984*b*). Helium is also known to be underabundant over the whole temperature domain of B and OB subdwarfs (Heber *et al.* 1984*b*; Heber and Hunger 1984).

It is very difficult to imagine a nuclear physics model to explain such a behavior. In particular, helium is generally produced, not destroyed, by stellar nuclear reactions. Diffusion has thus been called upon to explain the helium deficiency in the B subdwarfs and, more recently, has also been invoked to explain the metal abundance peculiarities. In particular, it has been repeatedly suggested (Baschek *et al.* 1982; Baschek, Höfflich, and Scholz 1982; Heber *et al.* 1984*a*, *b*) that the large Si underabundance in the hotter objects could be due to a reduced radiative acceleration on that element, which is mainly in a rare gas configuration in the atmosphere. Silicon would then settle gravitationally, and disappear from the surface.

As part of an ongoing investigation of the atmospheric properties of hydrogen-rich subdwarfs, we present here the first results of a study of diffusion processes in the envelopes of B and OB subdwarfs. In § II, it is shown that, in the absence of competing processes, *diffusion is not expected to lead to the observed* Si *underabundances.* The radiative acceleration on Si is much too large in the atmospheric region of such stars to allow large underabundances to develop. This leads us to consider additional particle transport processes in the envelope of sdB stars. In § III, we study how a weak ($\dot{M} < 10^{-14}\ M_\odot\ \mathrm{yr}^{-1}$), as yet undetectable, mass loss can affect the abundance anomalies created by diffusion.

II. THE PARAMETER-FREE MODEL FOR THE SILICON ABUNDANCE

In the absence of turbulence, meridional circulation, stellar winds, and magnetic fields, it is possible to make parameter-free calculations of the silicon abundance expected in hydrogen-rich subdwarfs. Atomic diffusion is then the only particle transport process. Its efficiency will depend very little on the original silicon abundance, since equilibrium abundances will be determined by the balance reached in the atmosphere between the radiative and gravitational accelerations. The equilibrium value is set by the abundance at which the lines saturate. The diffusion velocity of a trace ion of charge Z and atomic mass A in a fully ionized hydrogen plasma is given by:

$$v_D = D_{12}\left[-\frac{\partial \ln c}{\partial r} - \left(A - \frac{Z}{2} - \frac{1}{2}\right)\frac{m_p g}{kT} + \frac{A m_p g_R}{kT}\right], \quad (1)$$

where c is the element concentration, g_R is the radiative acceleration, m_p is the proton mass, and D_{12} is the atomic diffusion coefficient. Thermal diffusion is not a dominant process in outer stellar atmospheres, and it is not discussed here although its small effects were included in our calculations. Even though the abundance gradient term plays a role in the equilibrium abundances, the major one is played by the g and the g_R terms. The particle transport velocity is zero for values of g_R that very nearly cancel the gravitational settling term. It is then possible to get a good approximation to the equilibrium abundances in stellar atmospheres by calculating the element abundance for which g_R nearly equals g. Calculations of radiative accelerations are shown in Figure 1*a* for Si in our reference model envelope at $T_e = 35{,}000$ K and $\log g = 5.5$. The curve labeled MCV[2] was calculated as described in Michaud *et al.* (1976). Those labeled PRESS and $\times 10$ were calculated as described in Michaud, Vauclair, and Vauclair (1983). They differ in the treatment of the pressure broadening. The curve labeled $\times 10$ corresponds to pressure-broadened widths that are 10 times those used for the curve labeled PRESS. The differences among the various curves give a measure of the effect uncertainties in the pressure broadening have on the radiative acceleration.

The most important result of the radiative acceleration calculations is that silicon is supported (i.e., $g_R > g$) *in the atmo-*

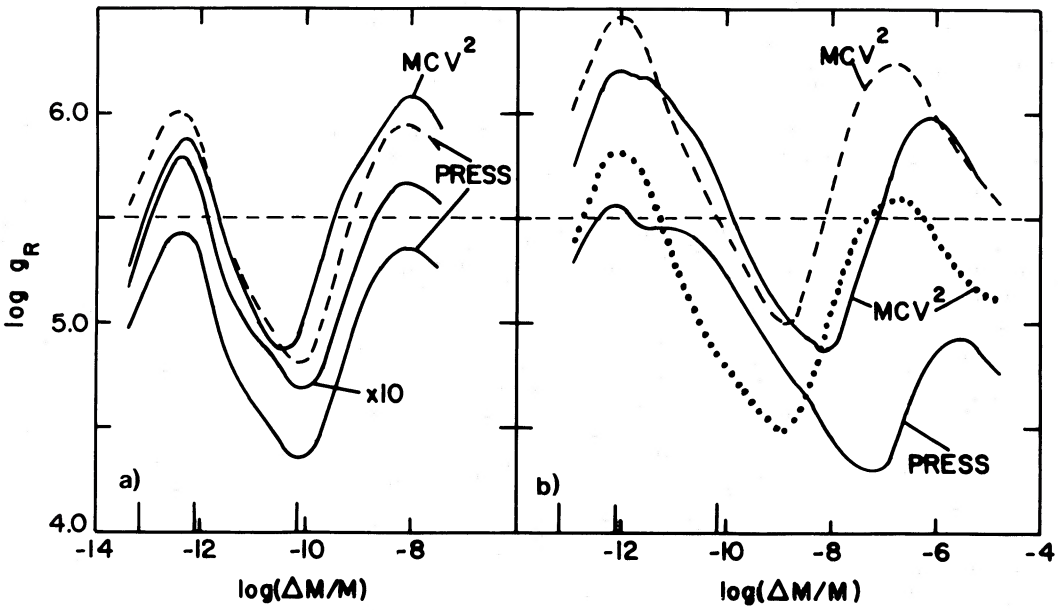

FIG. 1.—(*a*) Radiative accelerations on silicon as a function of depth in an envelope model at T_e = 35,000 K, log g = 5.5. The solid lines represent calculations performed for a solar silicon abundance, the dashed line for an abundance 0.1 the solar value. MCV^2 and PRESS indicate calculations performed following Michaud *et al.* (1976) and Michaud, Vauclair, and Vauclair (1983), respectively. The label × 10 indicates calculations similar to those labeled PRESS, but with pressure widths arbitrarily increased by a factor of 10. The horizontal dashed line indicates the surface gravity of the model, and the long tick marks on the bottom axis indicate Rosseland optical depths of, from left to right, 10^{-2}, 1, and 10^2. (*b*) Radiative accelerations on carbon (*dashed and dotted lines*) and nitrogen (*solid lines*) in the same envelope model as in (*a*). The dotted line represents calculations performed for a solar carbon value, the dashed line, for an abundance 0.1 the solar value. The labels MCV^2 and PRESS have the same meanings as in (*a*).

sphere for abundances much larger than the 10^{-5} solar which is suggested by the observations. This result holds well outside of the error bars of the radiative acceleration calculations. *The large dip in the radiative accelerations, which is due to the rare gas configuration of* Si, *occurs below the atmosphere:* even though Si is 50% of the time in the rare gas configuration while in the atmosphere, this only reduces the radiative acceleration by less than a factor of 2, while a reduction by a factor of 100 is needed for Si not to be more abundant than observed. For a reduction of the radiative acceleration by a factor of 100, silicon must be at least 99% of the time in the form of the rare gas. This value is even a lower limit, because of the reduced effects of saturation as the Si IV abundance decreases with increasing ionization. While silicon is already partially in the form of the noble gas, Si V, in the atmosphere, it is only much deeper that it is sufficiently in that form to cause a large enough reduction of the radiative acceleration. Indeed, in the line forming region, g_R has a local maximum since that is where it is the least in the rare gas form; silicon is further ionized below, by the increasing temperature, and above, by the reduced electron density. As can be seen from Figure 1*a*, the radiative acceleration on Si becomes, in the most unfavorable case (labeled PRESS), equal to gravity in the line forming region for an underabundance significantly less than by a factor of 10. *In the absence of competing processes, diffusion cannot account for the large underabundances of silicon observed in the hotter hydrogen-rich subdwarfs.*

The radiative accelerations on C and N are shown in Figure 1*b*. They both have a relative maximum in the atmospheric region of the envelope. However, these peaks are broader than those of Si (Fig. 1*a*), and the minima of g_R occur deeper in the envelope. These details of the variation of g_R in the envelope will be seen below to play an important role in the determination of the atmospheric abundances of the elements.

Calculations (not shown here) of radiative accelerations in a grid of model envelopes covering the range T_e = 20,000–50,000 K and log g = 5.0–6.0 confirm that our result holds throughout the domain where the Si underabundances are observed. Because diffusion provides a natural explanation for the observed helium underabundances, we feel that it is premature to discard it as the explanation of the metal abundance anomalies. We choose, rather, to investigate the abundances brought about by diffusion in the presence of a competing particle transport process, a weak stellar wind.

III. UNDERABUNDANCES AND MASS LOSS

In the presence of a mass-loss rate of $\sim 10^{-14}\ M_\odot\ \mathrm{yr}^{-1}$, the matter that was initially in the region where the radiative acceleration on Si is smaller than gravity ($\Delta M/M = 10^{-10}$) finds itself at the surface after $\sim 10^4$ yr. The silicon abundance at the surface now reflects processes that were occurring deeper in the star at an earlier stage, and, as we show below, large element underabundances are then possible.

The calculations of element separation in the presence of mass loss were carried out as described in Michaud *et al.* (1983), to which the reader is referred for details. One change was made to the method of calculations. Where the total transport velocity changes sign, the method used in Michaud *et al.* for heavy elements cannot be used, and one must instead use the detailed solution as was done there for helium. This method of solution was adapted to heavy elements. Details are given elsewhere (Michaud and Charland 1985), where the same method is applied to a model of λ Bootis stars. We assume here that no chemical separation is occurring in the stellar wind.

The results of these time-dependent calculations are shown in Figure 2. The left panel shows a snapshot of the Si concentration profile in the envelope, reached $\sim 6.5 \times 10^4$ yr after turning on a mass loss of $2.5 \times 10^{-15}\ M_\odot\ \mathrm{yr}^{-1}$. In first

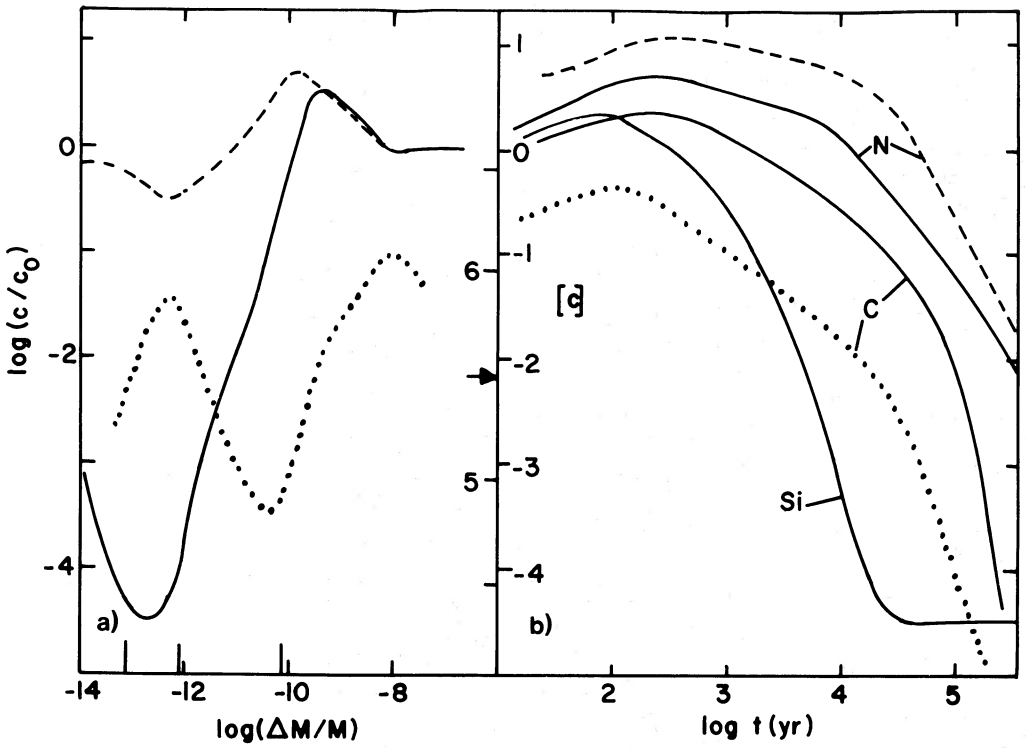

FIG. 2.—(*a*) Silicon concentration profile as a function of mass in the envelope $\sim 6.5 \times 10^4$ yr after the onset of mass loss. The model is for $T_e = 35{,}000$ K, $\log g = 5.5$. Two cases are presented: $\dot{M} = 2.5 \times 10^{-15}\ M_\odot\ \mathrm{yr}^{-1}$ (*solid line*) and $\dot{M} = 10^{-14}\ M_\odot\ \mathrm{yr}^{-1}$ (*dashed line*). The term c_0 is the initial silicon abundance, here taken to be the solar value. Also superposed, as a dotted line, is the radiative acceleration (g_R) on silicon, taken from Figure 1*a* (curve labeled MCV[2]). The shape of g_R at the epoch considered is qualitatively similar. The scale for g_R is on the right, that for $\log(c/c_0)$, on the left. The arrow indicates the surface gravity of the model. On the horizontal axis, the three long tick marks indicate Rosseland optical depths of, from left to right, 10^{-2}, 1, and 10^2. (*b*) Logarithmic abundances with respect to the solar values, [*c*], as a function of time in the photosphere ($\tau_{\mathrm{Ross}} = 0.17$) of our envelope model ($T_e = 35{,}000$ K, $\log g = 5.5$). The solid curves are for C, N, and Si with initial solar abundances: the dashed and dotted curves are for *N* with an initial abundance 4 times the solar value, and for *c* with an abundance one-tenth the solar value, respectively. For this mass-loss rate, the abundances reached on a time scale of $\sim 10^5$ yr are in good agreement with the observationally determined values (see text).

approximation, the calculated space distribution can be interpreted using the steady state element conservation equation

$$\nabla[cn_{\mathrm{H}}(v_w + v_D)] = 0\ , \qquad (2)$$

where v_w is the wind velocity and n_{H}, the hydrogen number density. In equation (2), the time derivative of c is neglected because the time changes in the atmosphere are governed, at such late times, by the rate of change in the deep envelope. As this rate is much slower than the atmospheric one, it contributes little to the conservation equation in the atmosphere. If one is interested only in trace elements in a hydrogen background, the wind velocity is determined by the continuity equation

$$4\pi r^2 m_p n_{\mathrm{H}} v_w = -\dot{M}\ , \qquad (3)$$

which assumes that the mass loss is not large enough to modify substantially the total mass of the star. Since equation (2) implies that the flux of Si is constant, while equation (3) states that the flux of H is constant, any change in v_D must be compensated by a change in c, the relative abundances of Si and H. If g_R increases outward, the diffusion velocity increases outward, so that c decreases to keep the flux constant (eq. [2]). In Figure 2*a*, the silicon abundance minimum near $\Delta M/M \approx 10^{-13}$ thus reflects the maximum in g_R(Si) at that location. This, it turns out, is also the region of line formation.

The large decrease in c between $\Delta M/M = 10^{-10}$ and $\Delta M/M = 10^{-11}$ is caused by the abundance gradient required, in equation (1), to maintain a constant outward flux of Si in the region where the radiative acceleration is smaller than gravity. If the mass-loss rate, or wind velocity, is increased by a factor of 4, this gradient rapidly goes to zero (see Fig. 2*a*). In that case, silicon does not have time to diffuse downward as the outflowing matter crosses the region of minimal radiative acceleration. Our results can be used to place an upper limit of $\sim 10^{-14}\ M_\odot\ \mathrm{yr}^{-1}$ on the mass-loss rate beyond which the observed large underabundance of Si does not materialize. We do not establish a lower limit. It would be set by the need to empty the region above the minimum in g_R(Si) in the stellar lifetime.

The resulting silicon abundance at the photosphere ($\tau_{\mathrm{Ross}} = 0.17$) of our model is displayed as a function of time in Figure 2*b* for a mass-loss rate of $2.5 \times 10^{-15}\ M_\odot\ \mathrm{yr}^{-1}$. At that rate, a steady state solution is reached after $\sim 10^5$ yr, with Si underabundant by over four orders of magnitude in the photosphere. The extent of this underabundance is in good agreement with the abundance ratios observed in hot sdB and sdOB stars. The Si abundance is not expected to increase again, unless the mass-loss rate changes.

The time-dependence of the C and N abundances in the photosphere is also shown in Figure 2*b*. Both abundances go through a maximum value followed, at later times, by a steady decrease. However, this decrease is delayed compared to that of the Si abundance. The reason is evident from Figure 1. The minimum in the radiative acceleration, and hence the concentration gradient, occurs deeper in the star for C than for Si, and still deeper for N. Thus the time scale for establishing this gradient, and for developing an underabundance at the photosphere, becomes increasingly longer. Two cases are

shown for both C and N, to cover approximately the range of abundances that may be produced if the outer region of such stars has gone through CNO burning. This may well have been the case, since the hot subdwarfs are believed to be evolved objects that have lost part of their envelope. The initial nitrogen abundance is then increased ($\times 4$), while the carbon abundance is decreased ($\times 0.1$) with respect to the solar values. Because of saturation effects on the radiative accelerations, anomalies take longer to appear if the initial abundance is increased.

Figure 2*b* suggests that, with a mass loss rate of 2.5×10^{-15} $M_\odot$ yr^{-1}, the following abundances are produced after 10^5 yr, if one starts with solar abundances: $[c(\mathrm{Si})] = -4.5$, $[c(\mathrm{C})] = -2.1$, $[c(\mathrm{N})] = -1.2$, where the square brackets denote logarithmic abundances with respect to the solar values. For smaller mass-loss rates, these abundances would be reached over longer time scales. If the original abundances of C and N are varied within the range expected from partial processing by the CNO cycle, then, after 10^5 yr, $[c(\mathrm{C})] = -4.0$, $[c(\mathrm{N})] = -0.6$. A variation of the original abundances within the limits allowed by partial CNO processing then allows us to reproduce the range of observed abundances of C, N, and Si.

IV. CONSTRAINTS ON MASS LOSS AND EVOLUTIONARY TIME SCALES

The inclusion of a weak mass loss in our description of the physical processes taking place in the envelopes of hot subdwarfs provides a natural explanation for the most significant abundance anomalies observed in these objects. In particular, the large silicon underabundance observed in the hot sdB stars can be explained *simultaneously* with the milder deficiency of carbon and the nearly normal nitrogen abundance. In the presence of such a mass loss, helium would also be underabundant by at least a factor of 10, in agreement with the observations. Even though we have not carried out calculations for He here, this can be inferred from the results of Michaud *et al.* (1983).

Our model may, eventually, be used to set constraints on the duration of the hot B subdwarf phase. If the evolutionary time scales were as long as $\sim 10^8$ yr (Heber *et al.* 1984*b*), large underabundances of both C and N would also materialize at the mass loss rate we have chosen. At that rate, the normal abundance of nitrogen observed in sdB stars probably excludes evolutionary time scales significantly longer than $\sim 10^6$ yr. However, this disagreement should be of little concern at this stage, as the exact value of this limit is expected to be dependent both on the mass loss rate and on the set of radiative accelerations used in the time-dependent calculations. As can be seen in Figure 1*b*, the position of the minimum of the radiative acceleration on nitrogen varies by a factor of 10 between the curve labeled MCV^2 and that labeled PRESS. The values of g_R used in Figure 2 are the MCV^2 values. Therefore, the time scale for the N underabundance to develop could be significantly longer if the other, presumably more accurate, values of g_R were used. Additional time-dependent abundance calculations with various sets of radiative accelerations and various mass-loss rates are needed to ascertain both the range of acceptable evolutionary time scales in the subdwarf phase, and the critical mass-loss rates beyond which no underabundances are produced.

We have assumed, in our time-dependent calculations, the existence of a weak stellar wind, an admittedly ad hoc hypothesis. However, there is no reason to believe that mass loss occurs only in those stars where it is large enough to be detected by current methods. There is no observational sign of a cutoff in mass-loss rates. Indeed, in the only star where small mass losses can be detected, the Sun, they are detected at the level of 10^{-14} $M_\odot$ yr^{-1}. The interaction between mass loss and superficial abundances may well thus become a measure of this important hydrodynamical parameter in other stars.

This work was supported in part by the NSERC Canada.

REFERENCES

Baschek, B., Höfflich, P., and Scholz, M. 1982, *Astr. Ap.*, **112**, 76.
Baschek, B., Kudritzki, R. P., Scholz, M., and Simon, K. P. 1982, *Astr. Ap.*, **108**, 387.
Baschek, B., and Norris, J. 1970, *Ap. J. Suppl.*, **19**, 327.
Baschek, B., Sargent, W. L. W., and Searle, L. 1972, *Ap. J.*, **173**, 611.
Heber, U., Hamann, W.-R., Hunger, K., Kudritzki, R. P., Simon, K. P., and Méndez, R. H. 1984*a*, *Astr. Ap.*, **136**, 331.
Heber, U., and Hunger, K. 1984, in *Proc. Fourth European IUE Conference* (ESA SP-218), p. 273.
Heber, U., Hunger, K., Jonas, G., and Kudritzki, R. P. 1984*b*, *Astr. Ap.*, **130**, 119.
Lamontagne, R., Wesemael, F., Fontaine, G., and Sion, E. M. 1985, *Ap. J.*, in press.
Michaud, G., and Charland, Y. 1985, in preparation.
Michaud, G., Charland, Y., Vauclair, S., and Vauclair, G. 1976, *Ap. J.*, **210**, 447.
Michaud, G., Tarasick, D., Charland, Y., and Pelletier, C. 1983, *Ap. J.*, **269**, 239.
Michaud, G., Vauclair, G., and Vauclair, S. 1983, *Ap. J.*, **267**, 256.

P. Bergeron, G. Fontaine, G. Michaud, and F. Wesemael: Département de Physique, Université de Montréal, C. P. 6128, Succ. A, Montréal, Québec, Canada H3C 3J7